

Periodicity in fields of elongating dunes

C. Gadal¹, C. Narteau¹, S. Courrech du Pont², O. Rozier¹ and P. Claudin³

¹Institut de Physique du Globe de Paris, UMR 7154 CNRS, Université de Paris, 75005 Paris, France

²Laboratoire Matière et Systèmes Complexes, UMR 7057 CNRS, Université de Paris, 75205 Paris, France

³Physique et Mécanique des Milieux Hétérogènes, UMR 7636 CNRS, ESPCI Paris and PSL Research University–Sorbonne Université–Université de Paris, 75005 Paris, France

ABSTRACT

Dune fields are commonly associated with periodic patterns that are among the most recognizable landscapes on Earth and other planetary bodies. However, in zones of limited sediment supply, where periodic dunes elongate and align in the direction of the resultant sand flux, there has been no attempt to explain the emergence of such a regular pattern. Here, we show, by means of numerical simulations, that the elongation growth mechanism does not produce a pattern with a specific wavelength. Periodic elongating dunes appear to be a juxtaposition of individual structures, the arrangement of which is due to regular landforms at the border of the field acting as boundary conditions. This includes, among others, dune patterns resulting from bed instability, or the crestline reorganization induced by dune migration. The wavelength selection in fields of elongating dunes therefore reflects the interdependence of dune patterns over the course of their evolution.

INTRODUCTION

Systematically highlighted by aerial photographs and satellite images, periodic geomorphological features have revealed the presence of dunes and atmospheric flows on planetary bodies including Earth, Mars, Titan, Pluto, and comets (McKee, 1979; Cutts and Smith, 1973; Ward et al., 1985; Lorenz et al., 2006; Bourke et al., 2010; Lorenz and Zimelman, 2014; Lucas et al., 2014; Jia et al., 2017; Diniega et al., 2017; Telfer et al., 2018). The origin of these periodic patterns is a central issue in dune physics and planetary sciences, along with the diversity of dune shapes, sizes, and orientations (Wasson and Hyde, 1983; Rubin and Hunter, 1987; Andreotti et al., 2009).

Under multidirectional flows, many dune fields with low sand availability exhibit linear dunes that extend for kilometers on nonerodible beds. These dunes result from an elongation growth mechanism leading to deposition at the dune tip of sediment transported along the crest under the action of reversing winds (Courrech du Pont et al., 2014; Gao et al., 2015b). While these elongating dunes can exist as isolated objects (Lucas et al., 2015), most fields of elongating dunes display a periodicity (Fig. 1). The origin of this periodicity has not yet been investigated or compared to pattern formation in zones where dunes can grow in height with

full sediment availability. A related point is thus how populations of dunes in transport- and sediment-limited conditions are independent based on current understanding of the emergence of dune wavelengths.

Periodic dune patterns are typically linked to the development of incipient bed forms due to an instability mechanism, which selects a characteristic length scale from the competition between destabilizing and stabilizing processes. The flat bed instability occurs in transport-limited conditions, where dunes arise from the interactions among turbulent flow, sediment transport, and topography at a wavelength λ_{\max} , for which the growth rate is maximal (Charru et al., 2013). Another instability occurs on transverse dunes migrating on a nonerodible bed. They break into a set of periodic barchan dunes with a size proportional to the height of the initial transverse dune (Reffet et al., 2010; Niiya et al., 2010; Parteli et al., 2011; Guignier et al., 2013). The collective dynamics of individual bed forms can also govern the development of patterns. In sediment-limited environments, these individual structures take the shape of barchans, domes, or star dunes according to the wind regime (Hersen, 2004; Zhang et al., 2012; Baddock et al., 2018; Gao et al., 2018). Whatever their shapes, as soon as they form populations, dunes interact by mass exchange induced either by collisions or sand flux. These interac-

tions generate a higher level of organization, with a characteristic size, frequently observed along the sand flow paths in dune corridors, chains, and clusters (Elbelrhiti et al., 2008; Worman et al., 2013; Génois et al., 2013a, 2013b). In all dune fields, independent of the origin of the pattern, nonlinear interactions also lead to an increase in dune amplitude and wavelength in space and time (Ewing and Kocurek, 2010; Valance, 2011; Gao et al., 2015a). While the smallest wavelengths are intrinsically associated with incipient bed forms, the coarsening process is restricted by boundary conditions, which can ultimately set the maximum length scales of the dune pattern.

By means of numerical simulations, we studied two independent configurations that produce periodic elongating dunes. We show that the spatial organization of these dunes is controlled by the geomorphological patterns from which they develop. The elongation growth mechanism does not itself select a characteristic wavelength but can be expressed from preexisting structures while retaining some of their properties. The periodic pattern is therefore inherited from past environments or specific boundary conditions upstream of the sand flow paths.

METHODS

We used a cellular automaton dune model that accounts for feedback mechanisms between the flow and the evolving bed topography (Rozier and Narteau, 2014). This approach has been shown to be efficient in modeling dunes in multidirectional wind regimes and is able to reproduce and quantify superimposed bed forms in dune fields (Zhang et al., 2012; Lü et al., 2017). The model parameters were the same as in Narteau et al. (2009), so that the model length and time units l_0 and t_0 were ≈ 0.5 m and $\approx 10^{-3}$ yr, respectively. Based on field observations, we implemented two specific configurations to generate periodic elongating dunes. In both cases, we considered a bidirectional wind regime with

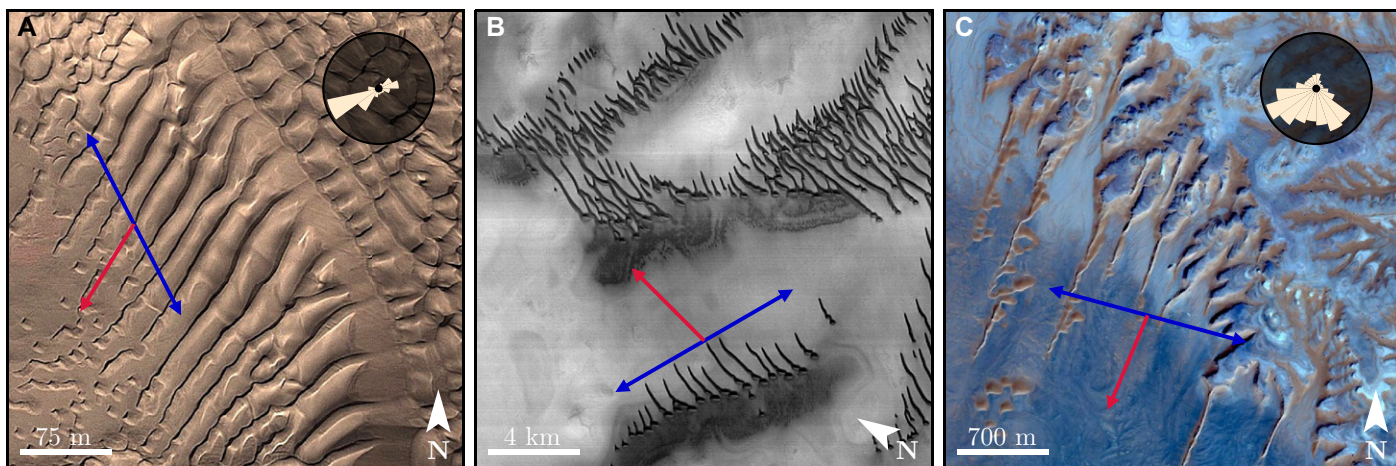


Figure 1. Periodic dune patterns. (A) Elongating dunes at bottom of avalanche slope, Taklamakan Desert, China ($37^{\circ}45'N$, $82^{\circ}36'E$). **(B)** Elongating dunes on Mars, Scandia Cavi ($78^{\circ}04'N$, $151^{\circ}10'W$). **(C)** Elongating dunes at bottom of erosion pattern, Rub' Al Khali Desert, Saudi Arabia ($10^{\circ}00'N$, $45^{\circ}40'E$). Arrows show dune orientations predicted from wind data on nonerodible bed (red) and sand layer (blue), following Courrech du Pont et al. (2014), except for Mars (B), where dune orientations were inferred from dune crests on satellite image. Insets show sand flux rose diagrams. Satellite images: Google™, Maxar Technologies (Colorado, USA), NASA/JPL/University of Arizona.

a divergence angle $\theta = 120^{\circ}$ and a constant wind strength (saturated flux over a flat sand bed $\approx 0.23l_0^2t_0^{-1}$). However, the duration of the winds was allowed to differ, and the transport ratio N was defined as the ratio between the time spent in the primary and secondary winds over a wind cycle T_w (Rubin and Hunter, 1987). Autocorrelation of the bed elevation was used to measure the elongation rate and the wavelength of the dune patterns.

In the first configuration, we focused on the development of dune patterns at the interface between a sediment layer of height $30l_0$ and a nonerodible bed. An avalanche slope made the transition between the two (Figs. 2 and 3). We used the simplest case of winds of equal duration ($N = 1$, $T_w = 100t_0$) with a resultant sand transport perpendicular to the avalanche slope. All dune orientations were aligned with the transport direction, and there was no lateral dune migration.

Along this direction, the output sand flux was lost (i.e., open conditions). Perpendicularly, the cellular space was made periodic to mimic an infinitely wide system.

In the second configuration, a sand bar of height H was placed over a nonerodible bed. We studied its migration when subjected to an asymmetric regime ($N = 3$, $T_w = 40t_0$) for which the dominant wind was perpendicular to the bar orientation (Fig. 4A). Along this direction, we kept open the output sand flux condition, preserving the periodicity in the perpendicular direction. As in a unidirectional wind regime, the bar migrates and can destabilize due to the lateral mass redistribution. Furthermore, in the presence of a secondary wind, elongating dunes can develop.

Finally, we interpreted field examples using the method described in Courrech du Pont et al. (2014). The predicted dune orientations were calculated from wind data provided by the ERA-Interim project or by local wind towers

(Fig. 1B). For the Martian example, they were measured from the dune crests on the satellite images (Fig. 1C).

RESULTS

Figures 2A–2C show the evolution of the bed forms at the border of the sediment layer. Incipient dunes develop from the flat bed instability on the sediment layer and the avalanche slope, and also elongate at the bottom of this lee face. Both dune types exhibit a regular pattern with well-defined wavelengths that connect with each other, as well as the same orientation due to the specific wind regime $N = 1$ (Fig. 2C). On the sediment layer, the dune wavelength starts from that of the most unstable mode associated with the bidirectional wind regime (Gadal et al., 2019). On the avalanche slope, the pattern wavelength starts at a slightly lower value, as does the one on the nonerodible ground. After a few wind cycles, both patterns connect through the avalanche slope, as the wavelengths become identical and then increase due to coarsening (Fig. 2D). The periodicity of the elongating dunes then appears to be controlled by that of the dunes on the sand layer. In addition, we observe that the pattern of the elongating dunes is directly impacted by the defects of the sediment layer pattern when the dunes reach the avalanche slope.

To test this control mechanism, we started simulations from a sediment layer with a sinusoidal elevation profile perpendicular to the resultant sand flux (Figs. 3A–3B). Figure 3C shows the wavelength of the dune patterns on both sides of the avalanche slope after 40 wind cycles with respect to the initial wavelength (λ_0). For λ_0 larger than λ_{\max} , there is perfect agreement between all these wavelengths (red part of Fig. 3C). As these large wavelengths are unstable with respect to the flat bed instability, the

initial pattern persists throughout the simulation, enforcing its periodicity onto the elongating dunes. For λ_0 smaller than λ_{\max} , however, the initial bed undulations are quickly replaced by those of the most unstable mode of the flat bed instability (blue part of Fig. 3C). As coarsening occurs along the resultant flux direction, the wavelength of the elongating dunes is a bit larger than the one measured on the sediment layer.

Figure 3D shows the elongation rate of the dunes developing at the bottom of the avalanche slope as a function of time. These measurements were done for three large wavelengths (red part in Fig. 3C). After a short transient time period of 5–10 wind cycles, all three elongation rates fluctuate around the same constant value. This duration corresponds to the time needed for the dunes at the base of the avalanche slope to reach the minimal size integrating the two winds. In the next phase, during which they elongate at a constant average rate, the dune tip periodically breaks, migrates, and disperses, explaining the observed variability. As no wavelength emerges faster than the others, the elongation mechanism does not select any length scale.

Using the second configuration, Figure 4A shows a migrating sandbar that becomes sinuous and ultimately breaks up into a periodic set of dunes. As in unidirectional wind regimes, the resulting wavelength of these dunes is determined by the height of the sandbar (Fig. 4). In bidirectional wind regimes, the crestline reorganization is not only related to the lateral redistribution of mass associated with the primary wind, but also to the superimposed bed forms that develop and migrate in an oblique direction with respect to the orientation of the sandbar (Courrech du Pont, 2015; Lü et al., 2017). Ultimately, the resulting periodic dunes also elongate under the action of the reversing winds (Fig. 4C), as in the experiments of Courrech du Pont et al. (2014).

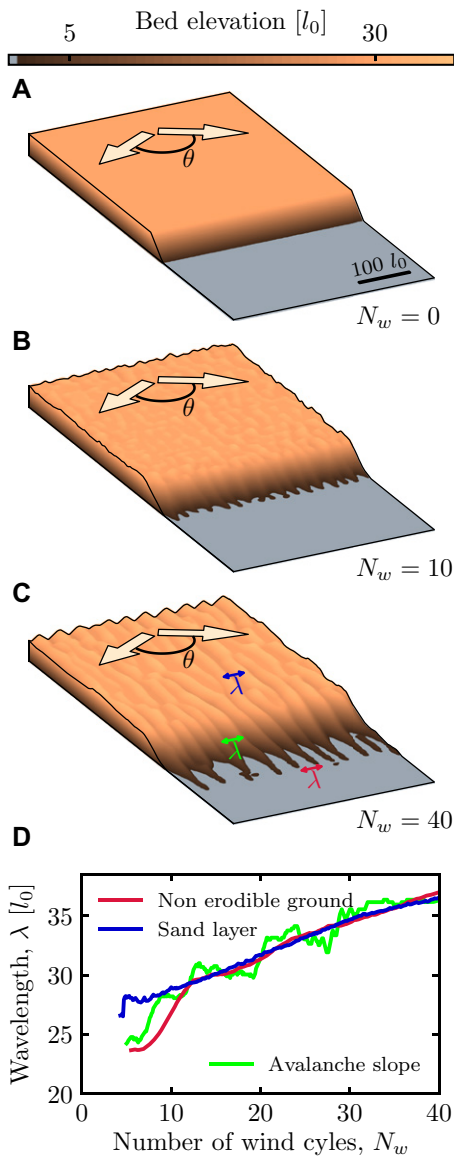


Figure 2. Dunes elongating at border of sediment layer. (A–C) Evolution of sediment bed in model. Nonerodible bed is shown in gray. (D) Wavelengths of pattern on sediment layer (blue), on avalanche slope (green), and on nonerodible (red) bed as function of time.

In multidirectional flows, the breakup of preexisting dunes is therefore another source of periodicity in fields of elongating dunes (Fig. 1B).

DISCUSSION

We identified two relevant length scales for dune growth in bidirectional wind regimes that are potential candidates for wavelength control in fields of elongating dunes. The first is the saturation length, associated with the spatial relaxation of transport in response to a bed perturbation (Andreotti et al., 2010). The second is proportional to $\sqrt{QT_w}$, where Q is the characteristic sand flux, and T_w is the duration of the wind cycle. As shown by Rozier et al. (2019), these two length scales control the minimal size and

the morphology of isolated elongating dunes. Nevertheless, our numerical simulations suggest that the periodicity in fields of elongating dunes comes from boundary and initial conditions rather than from length scales inherent to the elongation mechanism. This is supported by the fact that the elongation rate is independent of the initial wavelength (Fig. 3D).

We then recognized in this process the importance of the migration of dunes from areas of high to low sediment availability. When these dunes eventually fall into an avalanche slope in the transition zone, they impose a periodic modulation at its base, from which elongating dunes can develop (Fig. 1A). Interestingly, avalanche processes, and especially sand spreading during granular flow, can also add a level of complexity. In our numerical simulations, high slip faces can act as a filter and prevent transmission of upstream dune patterns that have too short an amplitude or wavelength down to the base of the avalanche slope. As a result, there is a range of wavelengths for

which information is lost in the avalanche slope (green part of Fig. 3C).

In addition, superimposed bed forms also appear and develop directly on avalanche slopes, which are areas of loose sand similar to a flat bed for oblique winds. In doing so, they also allow the elongation of periodic dunes at the base. Finally, multidirectional wind regimes more complex than the simplest symmetric bidirectional case studied in Figures 2 and 3 would induce an upstream dune orientation oblique to the avalanche slope. As a consequence, under natural conditions, we would expect additional geometric factors to be involved in the relation between the wavelength of the upstream bed forms and that of the elongating dunes.

Although the periodicity of many fields of elongating dunes appears to be governed by upstream dune patterns along the sand flow path, it can also be attributed to other spatially periodic landscapes. For example, channel formation and river erosion can lead to evenly spaced ridges and valleys (Fig. 1C). This could naturally give

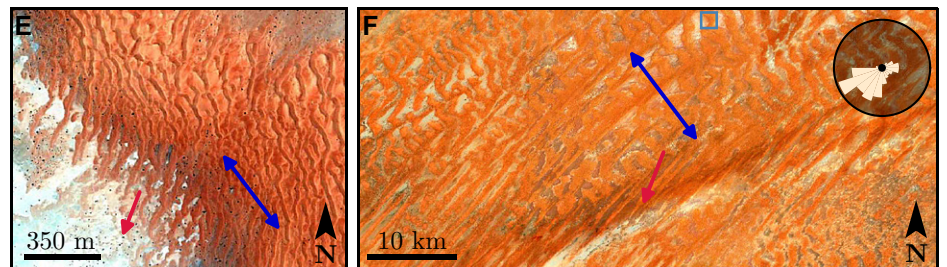
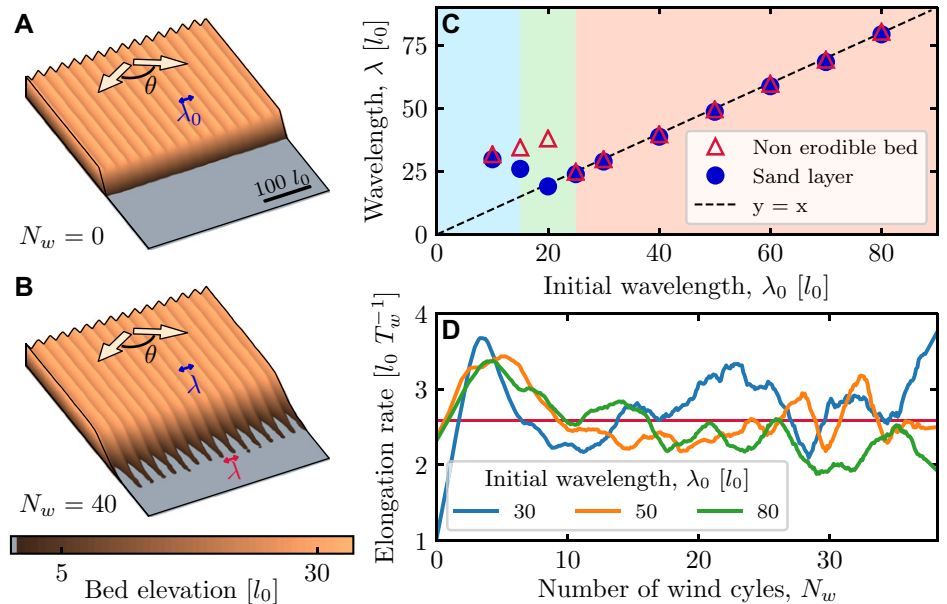


Figure 3. Dunes elongating at border of sinusoidal sediment layer. (A–B) Evolution of sediment bed in model for initial wavelength $\lambda_0 = 30l_0$. (l_0 —model length unit). (C) Wavelengths of pattern on sediment bed (blue) and on nonerodible bed (red) after 40 wind cycles as function of imposed wavelength λ_0 . (D) Elongation rate of dunes as function of time for different imposed wavelengths. Red line shows average value. (E–F) Field examples at small (E) and large (F) scales in western Sahara, Mauritania ($18^{\circ}11'N$, $14^{\circ}30'W$). Blue square is location of E on F. Arrows show dune orientations predicted from wind data on nonerodible bed (red) and sand layer (blue) following Courrech du Pont et al. (2014). Insets show sand flux rose diagrams. Satellite images: Google™, Maxar Technologies (Colorado, USA), Landsat/Copernicus.

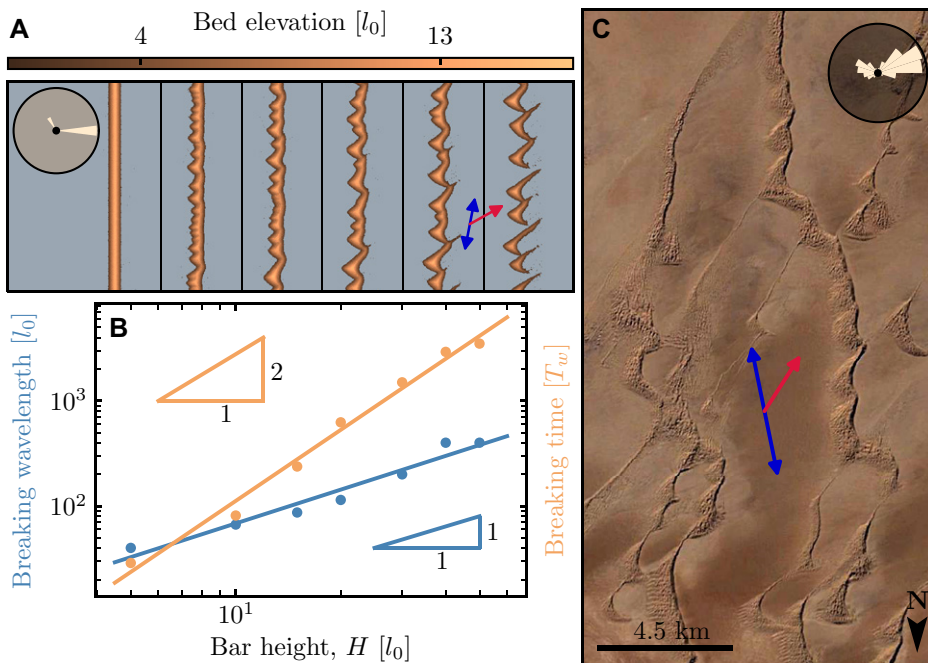


Figure 4. Breakup of a sandbar in bidirectional wind regime. (A) Evolution of a sandbar during its migration (corresponding number of wind cycles: $N_w = 0, 150, 225, 335, 400, 580$). (B) Wavelength of dune pattern and migration time as function of initial height of bar, measured at breaking. Points are numerical results, and lines are best linear fits. (C) Field example in Kavir Desert, Iran ($34^{\circ}06'N, 53^{\circ}40'E$). Arrows show dune orientations predicted from wind data on nonerodible bed (red) and sand layer (blue) following Courrech du Pont et al. (2014). Insets show sand flux rose diagrams. Satellite images: Google™, Maxar Technologies (Colorado, USA).

rise to a new type of interaction between eolian and fluvial systems in dryland environments (Bullard and Livingstone, 2002).

In modern sand seas, large numbers of extremely regular fields of elongating dunes have giant sizes, i.e., with a kilometer-scale spacing (Andreotti et al., 2009). Although we mainly addressed small- and medium-sized dunes in our numerical simulations, our results suggest that boundary conditions determine the periodicity of elongating dunes at any scale. When the dunes at the border have reached their giant size, the wavelength of the elongating dunes must adapt accordingly, preserving the periodicity along the sand flow paths (see Figs. 3E–3F). However, long-term interactions between elongating linear dunes and the resulting auto-organization require more investigation. In particular, dunes exchange sand by means of lateral fluxes, which make them expand longer (Rozier et al., 2018). Whether this process acts as a stabilizing or a destabilizing mechanism for the pattern is an open question.

More generally, our results illustrate how the transmission of the pattern at the border of dune fields exerts a spatio-temporal control on the geomorphology of the landscape along the sand flow path. Since any change at the border could be traced farther downwind over time, the observed dune morphodynamics could provide information about upstream dune patterns or past environments. They introduce a long-term memory into the migrating dune system. The

propagative aspect of the dynamics of the pattern is also apparent in the presence of an obstacle or in the elimination of defects. Because the density of defects is lower in fields of elongating dunes (Day and Kocurek, 2018), periodic patterns emerge more easily, even if they only develop under specific boundary conditions. On Earth, but also on other planetary bodies, these dynamic aspects can now be treated more carefully at the scale of major sand seas to learn more about the long-term evolution of arid landscapes and the variety of dune field patterns.

ACKNOWLEDGMENTS

We acknowledge financial support from the Univ-EarthS LabEx program of Sorbonne Paris Cité (grants ANR-10-LABX-0023 and ANR-11-IDEX-0005-02) and the French National Research Agency (grant ANR-17-CE01-0014/SONO). Clément Narteau acknowledges support from the National Science Center of Poland (grant 2016/23/B/ST10/01700).

REFERENCES CITED

Andreotti, B., Fourrière, A., Ould-Kaddour, F., Murray, B., and Claudin, P., 2009, Giant aeolian dune size determined by the average depth of the atmospheric boundary layer: *Nature*, v. 457, p. 1120, <https://doi.org/10.1038/nature07787>.
 Andreotti, B., Claudin, P., and Pouliquen, O., 2010, Measurements of the aeolian sand transport saturation length: *Geomorphology*, v. 123, p. 343–348, <https://doi.org/10.1016/j.geomorph.2010.08.002>.
 Baddock, M., Nield, J., and Wiggs, G., 2018, Early-stage aeolian protodunes: Bedform development and sand transport dynamics: *Earth Surface Processes and Landforms*, v. 43, p. 339–346, <https://doi.org/10.1002/esp.4242>.

Bourke, M.C., Lancaster, N., Fenton, L.K., Parteli, E., Zimelman, J., and Radebaugh, J., 2010, Extraterrestrial dunes: An introduction to the special issue on planetary dune systems: *Geomorphology*, v. 121, p. 1–14, <https://doi.org/10.1016/j.geomorph.2010.04.007>.
 Bullard, J., and Livingstone, I., 2002, Interactions between aeolian and fluvial systems in dryland environments: *Area*, v. 34, p. 8–16, <https://doi.org/10.1111/1475-4762.00052>.
 Charru, F., Andreotti, B., and Claudin, P., 2013, Sand ripples and dunes: *Annual Review of Fluid Mechanics*, v. 45, p. 469–493, <https://doi.org/10.1146/annurev-fluid-011212-140806>.
 Courrech du Pont, S., 2015, Dune morphodynamics: *Comptes Rendus Physique*, v. 16, p. 118–138, <https://doi.org/10.1016/j.crhy.2015.02.002>.
 Courrech du Pont, S., Narteau, C., and Gao, X., 2014, Two modes for dune orientation: *Geology*, v. 42, p. 743–746, <https://doi.org/10.1130/G35657.1>.
 Cutts, J., and Smith, R., 1973, Eolian deposits and dunes on mars: *Journal of Geophysical Research*, v. 78, p. 4139–4154, <https://doi.org/10.1029/JB078i020p04139>.
 Day, M., and Kocurek, G., 2018, Pattern similarity across planetary dune fields: *Geology*, v. 46, p. 999–1002, <https://doi.org/10.1130/G45547.1>.
 Diniega, S., Kreslavsky, M., Radebaugh, J., Silvestro, S., Telfer, M., and Tirsch, D., 2017, Our evolving understanding of aeolian bedforms, based on observation of dunes on different worlds: *Aeolian Research*, v. 26, p. 5–27, <https://doi.org/10.1016/j.aeolia.2016.10.001>.
 Elbelrhiti, H., Andreotti, B., and Claudin, P., 2008, Barchan dune corridors: Field characterization and investigation of control parameters: *Journal of Geophysical Research—Earth Surface*, v. 113, F02S15, <https://doi.org/10.1029/2007JF000767>.
 Ewing, R., and Kocurek, G., 2010, Aeolian dune-field pattern boundary conditions: *Geomorphology*, v. 114, p. 175–187, <https://doi.org/10.1016/j.geomorph.2009.06.015>.
 Gadal, C., Narteau, C., Courrech du Pont, S., Rozier, O., and Claudin, P., 2019, Incipient bedforms in a bidirectional wind regime: *Journal of Fluid Mechanics*, v. 862, p. 490–516, <https://doi.org/10.1017/jfm.2018.978>.
 Gao, X., Narteau, C., and Rozier, O., 2015a, Development and steady states of transverse dunes: A numerical analysis of dune pattern coarsening and giant dunes: *Journal of Geophysical Research—Earth Surface*, v. 120, p. 2200–2219, <https://doi.org/10.1002/2015JF003549>.
 Gao, X., Narteau, C., Rozier, O., and Courrech Du Pont, S., 2015b, Phase diagrams of dune shape and orientation depending on sand availability: *Scientific Reports*, v. 5, p. 14677, <https://doi.org/10.1038/srep14677>.
 Gao, X., Gadal, C., Rozier, O., and Narteau, C., 2018, Morphodynamics of barchan and dome dunes under variable wind regimes: *Geology*, v. 46, p. 743–746, <https://doi.org/10.1130/G45101.1>.
 Géniois, M., Courrech Du Pont, S., Hersen, P., and Grégoire, G., 2013a, An agent-based model of dune interactions produces the emergence of patterns in deserts: *Geophysical Research Letters*, v. 40, p. 3909–3914, <https://doi.org/10.1002/grl.50757>.
 Géniois, M., Courrech Du Pont, S., Hersen, P., and Grégoire, G., 2013b, Spatial structuring and size selection as collective behaviours in an agent-based model for barchan fields: *European Physical Journal B: Condensed Matter and Complex Systems*, v. 86, p. 447, <https://doi.org/10.1140/epjb/e2013-40710-2>.
 Guignier, L., Niiya, H., Nishimori, H., Lague, D., and Valance, A., 2013, Sand dunes as migrating strings: *Physical Review E*, v. 87, p. 052206, <https://doi.org/10.1103/PhysRevE.87.052206>.

- Hersen, P., 2004, On the crescentic shape of barchan dunes: *European Physical Journal B: Condensed Matter and Complex Systems*, v. 37, p. 507–514, <https://doi.org/10.1140/epjb/e2004-00087-y>.
- Jia, P., Andreotti, B., and Claudin, P., 2017, Giant ripples on comet 67P/Churyumov–Gerasimenko sculpted by sunset thermal wind: *Proceedings of the National Academy of Sciences of the United States of America*, v. 114, p. 2509–2514, <https://doi.org/10.1073/pnas.1612176114>.
- Lorenz, R., et al., 2006, The sand seas of Titan: *Cassini* radar observations of longitudinal dunes: *Science*, v. 312, p. 724–727, <https://doi.org/10.1126/science.1123257>.
- Lorenz, R.D., and Zimbelman, J.R., 2014, *Dune Worlds: How Windblown Sand Shapes Planetary Landscapes*: Berlin, Springer Science & Business Media, <https://doi.org/10.1007/978-3-540-89725-5>.
- Lü, P., Narteau, C., Dong, Z., Rozier, O., and Courrech du Pont, S., 2017, Unravelling raked linear dunes to explain the coexistence of bedforms in complex dunefields: *Nature Communications*, v. 8, p. 14239, <https://doi.org/10.1038/ncomms14239>.
- Lucas, A., et al., 2014, Growth mechanisms and dune orientation on Titan: *Geophysical Research Letters*, v. 41, p. 6093–6100, <https://doi.org/10.1002/2014GL060971>.
- Lucas, A., Narteau, C., Rodriguez, S., Rozier, O., Callot, Y., Garcia, A., and Courrech du Pont, S., 2015, Sediment flux from the morphodynamics of elongating linear dunes: *Geology*, v. 43, p. 1027–1030, <https://doi.org/10.1130/G37101.1>.
- McKee, E., 1979, Introduction to a study of global sand seas, in McKee, E.D., ed., *A Study of Global Sand Seas*: U.S. Geological Survey Professional Paper 1052, p. 1–19, <https://doi.org/10.3133/pp1052>.
- Narteau, C., Zhang, D., Rozier, O., and Claudin, P., 2009, Setting the length and time scales of a cellular automaton dune model from the analysis of superimposed bed forms: *Journal of Geophysical Research—Earth Surface*, v. 114, F03006, <https://doi.org/10.1029/2008JF001127>.
- Niiya, H., Awazu, A., and Nishimori, H., 2010, Three-dimensional dune skeleton model as a coupled dynamical system of two-dimensional cross sections: *Journal of the Physical Society of Japan*, v. 79, p. 063002, <https://doi.org/10.1143/JPSJ.79.063002>.
- Parteli, E., Andrade, J., Jr., and Herrmann, H., 2011, Transverse instability of dunes: *Physical Review E*, v. 107, p. 188001, <https://doi.org/10.1103/PhysRevLett.107.188001>.
- Reffet, E., Courrech du Pont, S., Hersen, P., and Douady, S., 2010, Formation and stability of transverse and longitudinal sand dunes: *Geology*, v. 38, p. 491–494, <https://doi.org/10.1130/G30894.1>.
- Rozier, O., and Narteau, C., 2014, A real-space cellular automaton laboratory: *Earth Surface Processes and Landforms*, v. 39, p. 98–109, <https://doi.org/10.1002/esp.3479>.
- Rozier, O., Narteau, C., Gadal, C., Claudin, P., and Courrech du Pont, S., 2019, Elongation and stability of a linear dune: *Geophysical Research Letters*, v. 46, <https://doi.org/10.1029/2019GL085147>.
- Rubin, D., and Hunter, R., 1987, Bedform alignment in directionally varying flows: *Science*, v. 237, p. 276–278, <https://doi.org/10.1126/science.237.4812.276>.
- Telfer, M., et al., 2018, Dunes on Pluto: *Science*, v. 360, p. 992–997, <https://doi.org/10.1126/science.aao2975>.
- Valance, A., 2011, Nonlinear sand bedform dynamics in a viscous flow: *Physical Review E*, v. 83, p. 036304, <https://doi.org/10.1103/PhysRevE.83.036304>.
- Ward, A., Doyle, K., Helm, P., Weisman, M., and Witbeck, N., 1985, Global map of eolian features on Mars: *Journal of Geophysical Research—Solid Earth*, v. 90, p. 2038–2056, <https://doi.org/10.1029/JB090iB02p02038>.
- Wasson, R., and Hyde, R., 1983, Factors determining desert dune type: *Nature*, v. 304, p. 337, <https://doi.org/10.1038/304337a0>.
- Worman, S., Murray, A., Littlewood, R., Andreotti, B., and Claudin, P., 2013, Modeling emergent large-scale structures of barchan dune fields: *Geology*, v. 41, p. 1059–1062, <https://doi.org/10.1130/G34482.1>.
- Zhang, D., Narteau, C., Rozier, O., and Courrech du Pont, S., 2012, Morphology and dynamics of star dunes from numerical modelling: *Nature Geoscience*, v. 5, p. 463–467, <https://doi.org/10.1038/ngeo1503>.

Printed in USA